IJPAS ISSN: 2149-0910 | INTERNATIONAL JOURNAL PURE AND APPLIED SCIENCES

Vol. 10(2); 309-324 (2024)
DOI: 10.29132/ijpas.1481272

Research Article

Changes on the Physical Structure Caused by the Advanced Grinding Process before Direct Reduction of Chalcophyrite Concentrate with Carbon

Mustafa BOYRAZLI [1], Elif ARANCI ÖZTÜRK [2,*], Selman YILMAZ [1], Mustafa SÜNER [1] Emrah ÇELİK [1], Güneş BAŞBAĞ [1]

Received: 09.05.2024

Accepted: 12.08.2024

[1] Firat University, Faculty of Engineering, Department of Metallurgical and Materials Engineering, Elazig, Türkiye, mboyrazli@firat.edu.tr, s_yilmaz230@hotmail.com, msnr023@gmail.com, emrahcelik@firat.edu.tr, gunesbasbag@gmail.com

[2] Balikesir University, Balikesir Vocational School, Department of Machine and Metal Technologies, Balikesir, Türkiye, elif.ozturk@balikesir.edu.tr

* Corresponding author

Abstract: After selecting the appropriate pyrometallurgical or hydrometallurgical methods according to the type of ore used in copper production, electrometallurgical refining processes are applied to reach the desired purity level. When mechanical activation processes are applied before reduction processes, they have changed the traditional workflow scheme in many processes by both shortening the process and reducing energy consumption. This study constitutes the first stage of the direct reduction of chalcopyrite in the presence of carbon and quicklime. The mixture consisting of biochar, quicklime and concentrated chalcopyrite was mixed in a stoichiometric ratio and over-ground in a spex type mill for different periods of time. Changes in the physical structure of the over-ground mixture were examined by XRD, SEM and EDX images. XRD images showed that there was a large amount of amorphization in the crystal structure as a result of excessive grinding of the material for 60 minutes. According to the DLS analysis results, it was observed that the grain size decreased to 5240 nm due to increasing grinding time.

Keywords: advanced grinding; biocoal; chalcopyrite; direct reduction; spex.

Kalkopirit Konsantresinin Karbon ile Direkt Redüksiyonundan Önce İleri Öğütme İşleminin Fiziksel Yapıda Oluşturduğu Değişimler

Özet: Bakır üretiminde kullanılan cevherin cinsine göre uygun pirometalurjik veya hidrometalurjik yöntemler seçildikten sonra istenilen saflık seviyesine ulaşmak için elektrometalurjik rafinasyon işlemleri uygulanır. Mekanik aktivasyon işlemleri redüksiyon işlemlerinden önce uygulanarak hem süreci kısaltıp hem de enerji tüketimini azaltarak birçok proseste geleneksel iş akış diyagramını değiştirmiştir. Bu çalışma, kalkopiritin karbon ve sönmemiş kireç varlığında doğrudan indirgenmesinin ilk aşamasını oluşturmaktadır. Stokiyometrik oranda karıştırılan biyokömür, kalkopirit konsantresi ve sönmemiş kireç spex tipi bir değirmende farklı sürelerde öğütülmüştür. Aşırı öğütülmüş karışımın fiziksel yapısındaki değişiklikler XRD, SEM ve EDX görüntüleri ile incelenmiştir. XRD görüntülerinde malzemenin 60 dakika boyunca aşırı öğütülmesi sonucu kristal yapısında büyük miktarda amorflaşma olduğu görülmüştür. DLS analiz sonuçlarına göre artan öğütme süresi ile birlikte tane boyutunun 5240 nm'ye kadar düştüğü gözlemlenmiştir.

Anahtar Kelimeler: biyokömür; doğrudan indirgeme; ileri öğütme; kalkopirit; spex.

1. Introduction

Copper, one of the few metals in metallic form that can be used directly in nature, was discovered in B.C. It has been used since the 8000s. The oldest known copper remains were found in Çatalhöyük in Central Anatolia, and it was first used alone and later in the form of tin alloy bronze or bronze. The first copper production in Anatolia dates back to B.C. It was started by the Assyrians in 2000 B.C. from the deposits in Elazığ-Maden [1]. Of the minerals used in copper production, approximately 50% is chalcosite (Cu_2S), 25% is chalcopyrite ($CuFeS_2$), 3% is enargite (Cu_3AsS_4), 1% is other sulfur minerals, 6-7% is native copper and 15% consists of oxide minerals. Copper ores found in nature generally contain gangue minerals. In order to be produced by pyrometallurgical or hydrometallurgical methods, gangue minerals are first removed and the grade of the ores is increased through ore preparation and enrichment processes. Pyrometallurgical methods (Figure 1) are applied to sulfide, oxide and native copper ores, and hydrometallurgical methods (Figure 2) are applied to low grade oxide copper ores. Pre-enrichment processes are similar in both copper production methods [2]. In the final stage, by applying electrometallurgical methods, the impure copper obtained by both methods is subjected to electrolytic refining and converted into pure cathode copper. While 80% of the world copper production is made by pyrometallurgical methods, the remaining part includes hydrometallurgical methods [3].

The conventional methods for the production of non-ferrous metals from mineral sulphides are based on two main pyrometallurgical principles. In one case, the mineral sulphides are dead roasted (i.e. a complete elimination of sulphur from the sulphides by converting them to metallic oxides) and then treated in a furnace to reduce the metal oxides to metal. Alternatively, if the sulphide concentrates are rich and fine, they are directly charged into the Flash Smelting Furnace to produce matte. In particular, the production of sulphurous Cu, Ni, Co and Pb metals by traditional pyrometallurgical methods involves different roasting, melting and conversion steps. The sulphur dioxide gas released during these steps causes major environmental problems. It is imperative to reduce sulphur dioxide emissions generated during pyrometallurgical processing of sulphurous ores [6-14]. Therefore, in recent years, many attempts have been made to develop new processes for the purification of copper sulphide concentrates that do not cause significant air pollution through SO_2 emissions [3, 15-17].

Mechanical activation, defined by Smekal as "a process that increases the ability of the solid to react", is widely used in extractive metallurgy. The advantages of mechanical activation include lowering reaction temperatures, increasing the amount and speed of solubility, formation of water-soluble substances, the need for a simpler and more economical reactor, and shorter reaction times [18].

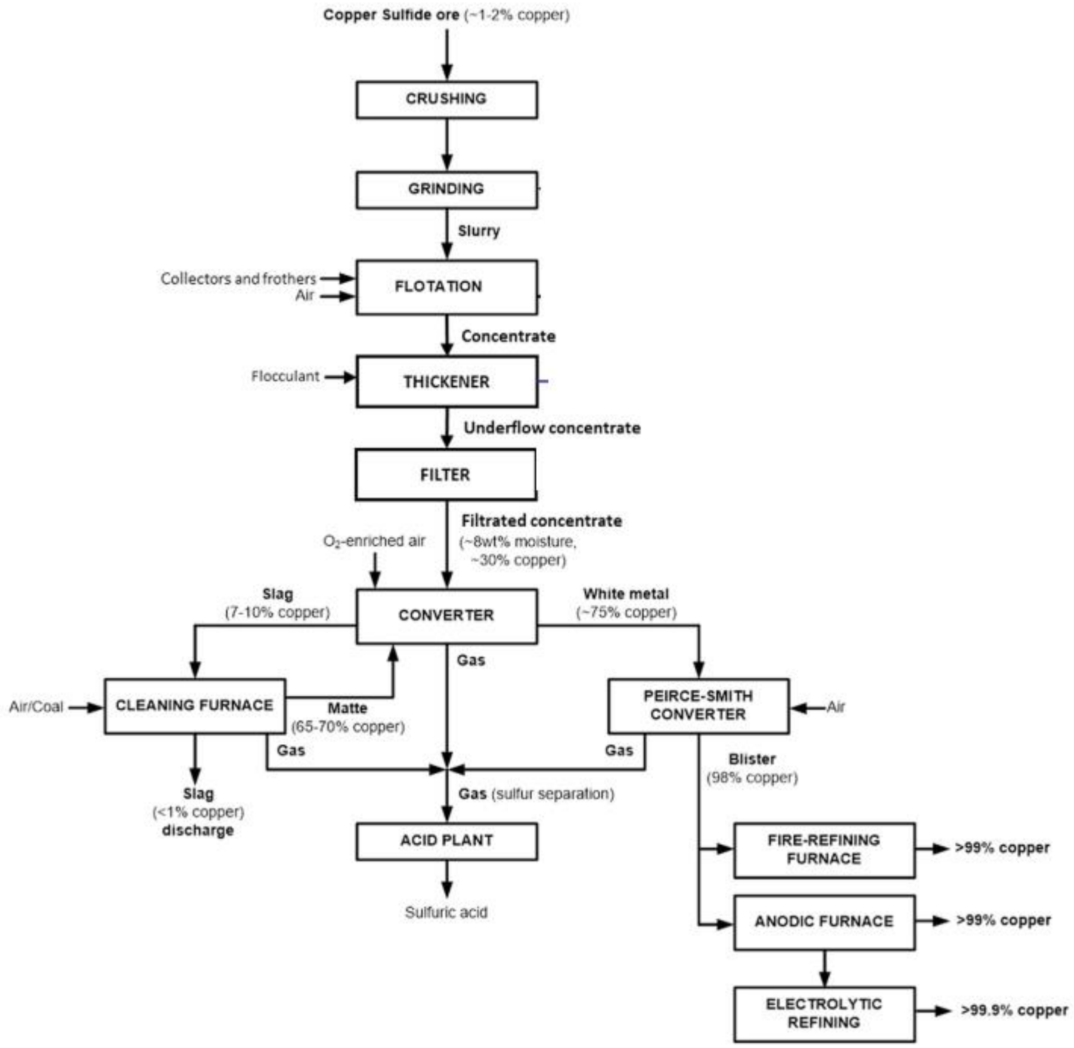

Figure 1. Pyrometallurgical copper production [4].

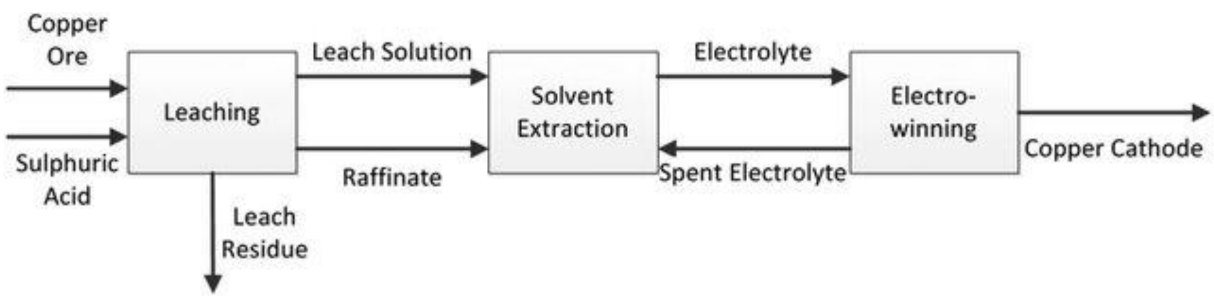

Figure 2. Hydrometallurgical copper production [5].

Mills used for advanced grinding; ball mill, planetary mill, vibrating mill, agitated ball mill (atriator), spindle mill and rolling mill. Mills used for advanced grinding are given schematically in Figure 3 [19].

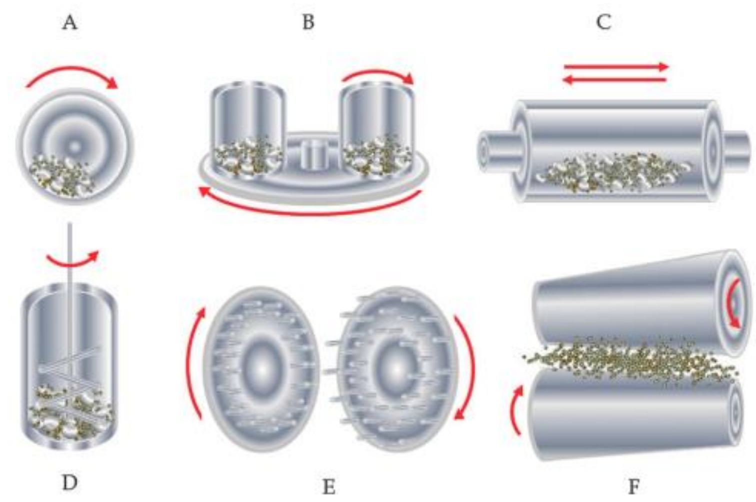

Figure 3. Mill Types Used for Advanced Grinding Process, A-Ball Mill, B-Planetary Mill, C-Vibrating Mill, D-Agitated Ball Mill (Atritor), E-Spindle Mill, F-Rolling Mill [19].

Mechanical activation process is a technique that has been applied at various stages of metal production processes from chrome [20], zinc [21], aluminum [22], manganese [18] and iron [23] ores and positive results have been obtained. The effect of mechanical activation on leaching processes in the production of copper ores by hydrometallurgical methods has been examined by many researchers [24-27].

Biomass is energy obtained from natural substances of plant or animal origin and causes less harm to the environment thanks to its low sulfur content. The ash produced by the combustion of biomass fuels is of a quality that can be used for agricultural purposes [23].

Almond is among the important hard-shelled fruits adapted to Turkey's climate structure. Almonds can be grown in almost every region of our country except the Eastern Black Sea coastal regions and high plateaus [28]. Various studies have been conducted to evaluate almond shells. Generally, studies involve the removal of heavy metals or dyes by producing activated carbon from almond shells [29, 30]. Its use in soilless vegetable cultivation [31], pyrolysis [32] and biochar production [33] are the search for new usage areas that attract attention.

In this article, we examined the effect of advanced grinding process, which is the first stage of our work to obtain directly reduced copper from chalcopyrite, change of the physical structure of mixture consisting of quicklime, chalcopyrite concentrate and biocoal.

2. Experimental Study

2.1. Material

In the studies, chalcopyrite concentrate obtained from Yıldızlar Holding A.Ş., located in Elazığ-Maden district, was used. In addition, purchased calcium oxide and almond shells containing 92.36% C and 0.018% S after at 700 ºC for 4 h carbonization were used as biocoal. ICP-MS analysis of the chalcopyrite concentrate used in ARGETEST laboratory is given in Table 1.

Table 1. *Chemical analysis of chalcopyrite concentrate*

Component	Amount	Component	Amount
Cu	19.03 (%)	Ag	12.06 (ppm)
Fe	33.32 (%)	Al	0.60 (%)
S	26.56 (%)	Co	1159.0 (ppm)

For advanced grinding processes, MTI Corporation SFM-3 Desk-Top High Speed Vibrating Ball Miller brand spex mill, shown in Figure 4 (a), was used. The spex chamber shown in Figure 4 (b), where the advanced grinding process is carried out, is a chamber specially manufactured from tungsten carbide with a depth of 56 mm, an inner diameter of 48 mm and a wall thickness of 7 mm. Steel balls with a diameter of 6 mm were used for advanced grinding.

The advanced grinding process was carried out with a powder/ball ratio of 1/20 so that the stoichiometrically prepared powders would fill one-third of the specimen chamber and 7.5 g of powder material (6,000 g CuFeS2 ore, 1.35 g CaO, 0.174 g C) and 150 g balls were weighed and placed in the specimen chamber. The advanced grinding process was determined as 15 min, 30 min, and 60 min.

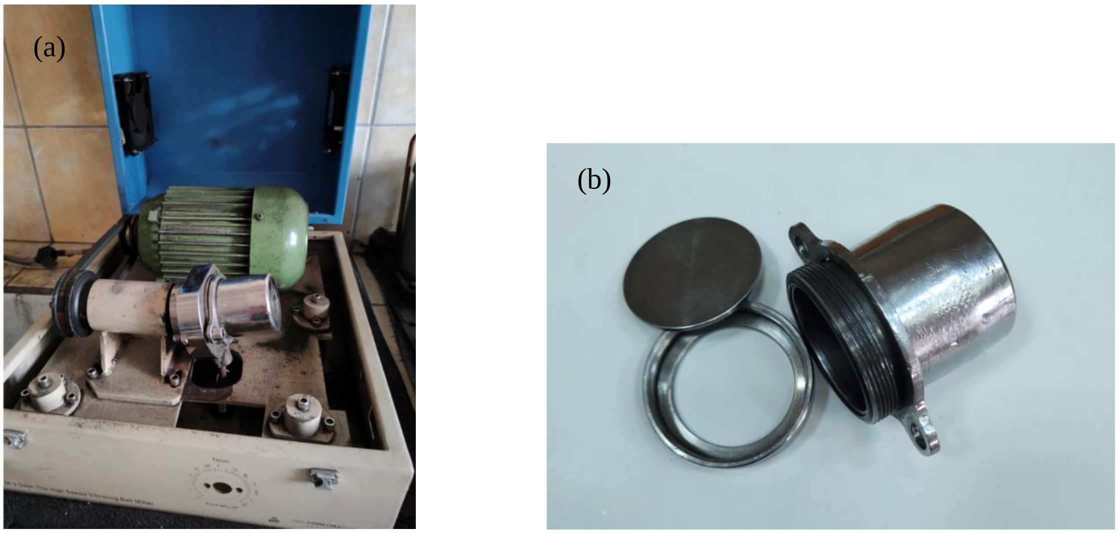

Figure 4. a) Spex mill, b) Spex chamber

After the advanced grinding process, the spex chamber was opened in the glove-box and the operations inside the box were carried out in a nitrogen gas atmosphere. Then the powders ground was taken out from the chamber in the glove-box and placed in zip lock bags. After further grinding, XRD analyses of both the ground samples and the original mixture were performed on a Rigaku Mini Flex 600 brand X-Ray Diffractometer.

After advanced grinding, thermal characterization experiments were carried out on the samples on a Shimadzu brand DTG-60AH model differential thermal analysis (DTA) device. TG/DTA analyses of the samples were performed by heating and cooling between 25-750 ºC, at a heating/cooling rate of 20 ºC/minute, in an air environment with a constant flow of 100 ml/minute.

Dynamic light scattering was used to determine the size distribution profile of small particles in solution. The Particle Sizing System NICOMP 380, a product of Nicomp, Santa Barbara, California, uses Dynamic Light Scattering (DLS) to obtain the particle size distribution for samples with particles ranging from 2 nm to 10 microns. Through the use of the proprietary Nicomp analysis algorithm, the 380 is able to analyse complex multi-modal distributions with the highest resolution and reproducibility available.

2.2. Method

Before starting the studies, the chalcopyrite concentrate was size analysed and it was determined that it had a grain size of -200 µm. Then, biocoal and CaO were pretreated to a size of -200 µm and experiments were started. In the study, biocoal, chalcopyrite concentrate and quicklime (CaO) were prepared in stoichiometric ratio according to the equation (2.1) given below and further grinding was carried out in the spex mill.

Before the grinding process, the powder mixture/ball ratio was determined as 1/20 and the mixture was prepared to fill one third of the spex chamber. Advanced grinding processes were carried out for 15 min, 30 min and 60 min. The product obtained after grinding was removed from the mill chamber in a glove-box, and the samples were named S-15, S-30 and S-60 depending on the grinding times. XRD, SEM and TG/DTA analyses of the obtained powders were performed.

$$CuFeS2(s) + 2CaO(s) + C(s) = Cu(s) + FeO(s) + 2CaS(s) + CO(g) \quad (2.1)$$

3. Results and Discussion

3.1. XRD and DLS Analyzes

XRD images of the advanced grinding and original mixture are given in Figure 5. Literature peak data of chalcopyrite are seen in Table 2.

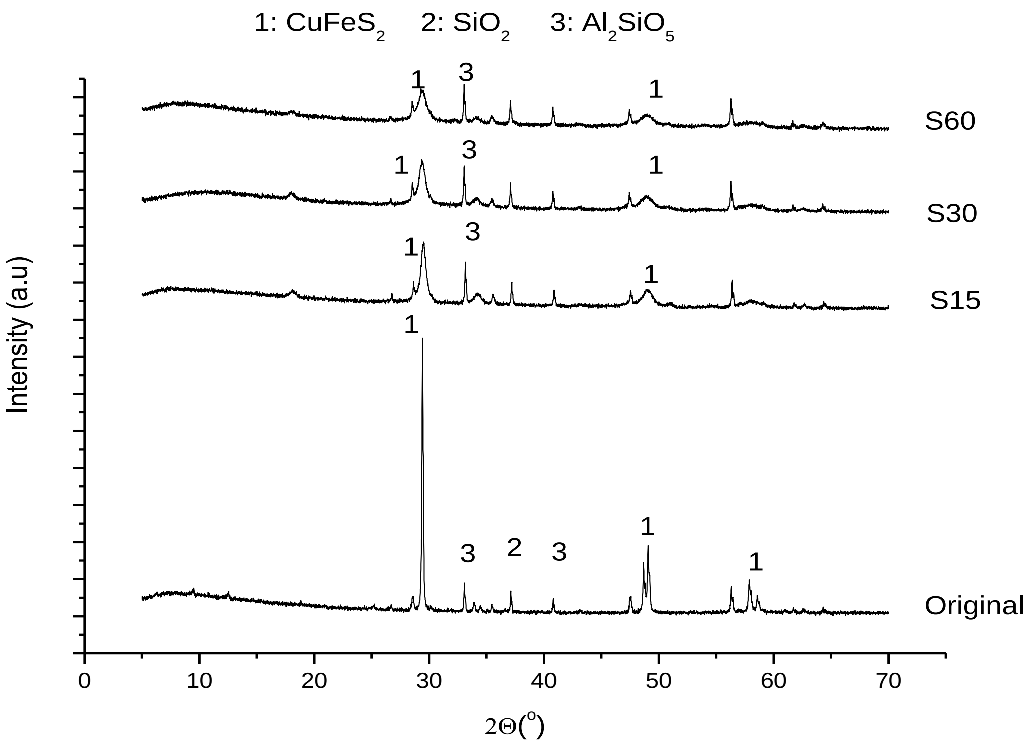

Figure 5. XRD images of the original mixture and the samples subjected to advanced grinding

Table 2. *XRD literature peak data of chalcopyrite [34].*

2 θ (°)	Intensity (au)	2 θ (°)	Intensity (au)
29.25	100.00	58.30	10.50
33.73	6.06	60.67	1.75
34.26	2.89	70.93	4.56
48.44	18.43	72.18	2.15
48.84	35.88	78.51	3.47
57.60	21.93	79.11	6.77

It can be seen that the dominant peak of chalcopyrite in the original sample decreases depending on the advanced grinding time. It can be said that nanostructures are formed by grinding processes in the mill chamber. Grinding temperature is expected to have a significant effect on the formation of these structures. During grinding, two types of temperature effects are generally taken into account: local temperatures resulting from the collision of the balls with each other and with the powder material, and temperatures created by the balls hitting the walls inside the chamber. It can be said that with the advanced grinding process, the powders in the concentrate are affected by these two temperatures and the crystal structure is deteriorated. However, it appears that the silicate peak is not due to the milling process and remains without amorphization. According to the Mohs hardness scale, the hardness of quartz is 7. However, the hardness of steel balls is around 5.5-6 and that of chalcopyrite is around 3.5-4. Considering the grinding environment and grinding materials selected for the advanced grinding process, the peaks of these minerals should not change after grinding. However, the chalcopyrite peak should be expected to decrease with grinding time. The analyses of Gaussian and Nicomp distributions in the water dispersion of advanced milled material as obtained by the Dynamic Light Scattering Method (DLS) is given Figures 6, 7 and 8.

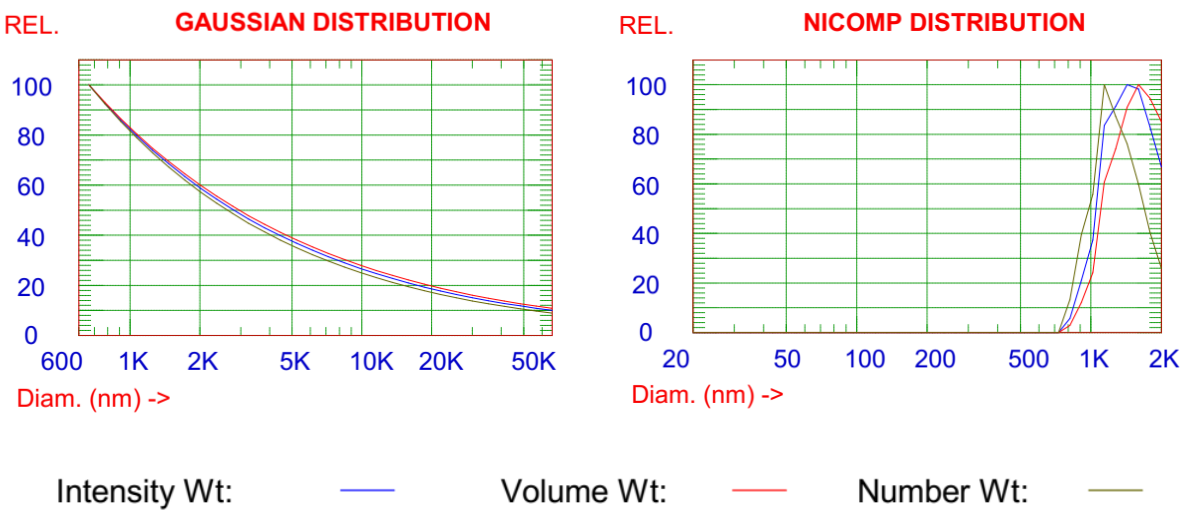

Cumulative Result:

25 % of distribution < 1294.7 nm | *50 % of distribution < 2552.8 nm*

75 % of distribution < 7104.2 nm | *80 % of distribution < 9460.0 nm*

Figure 6. DLS analysis of the mixture subjected to 15 minutes of advanced grinding

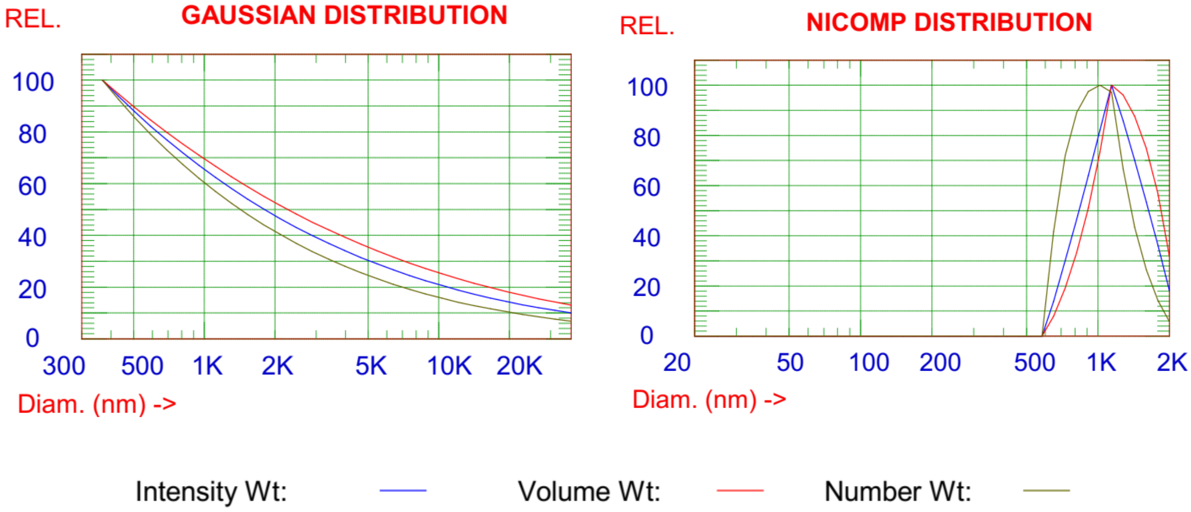

Cumulative Result:

25 % of distribution < 728.2 nm | *50 % of distribution < 1444.7 nm*

75 % of distribution < 3961.9 nm | *80 % of distribution < 5240.2 nm*

Figure 7. DLS analysis of the mixture subjected to 30 minutes of advanced grinding

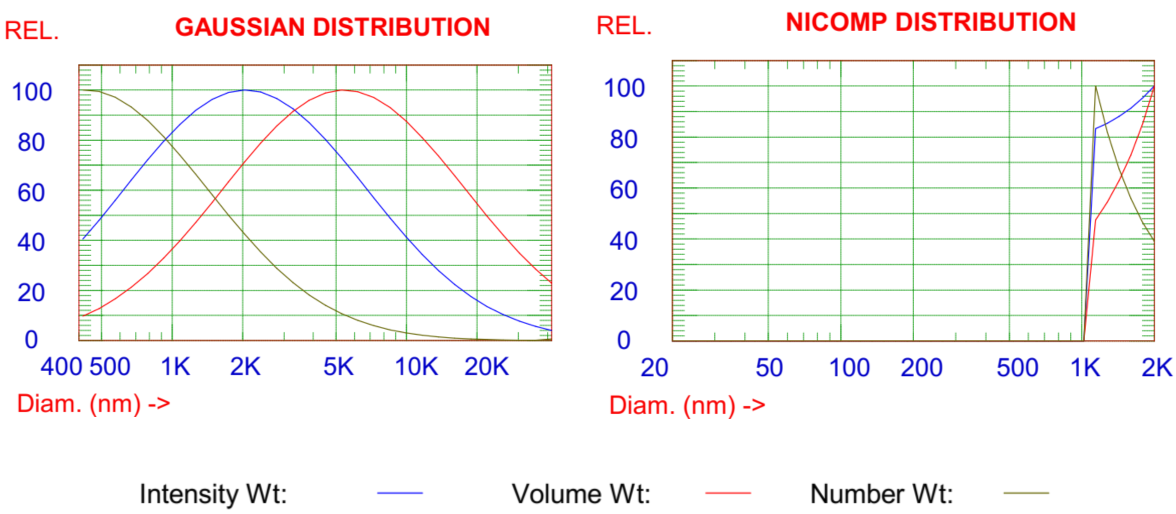

Cumulative Result:

25 % of distribution < 1230.8 nm | *50 % of distribution < 2410.7 nm*

75 % of distribution < 5020.4 nm | *80 % of distribution < 6042.9 nm*

Figure 8. DLS analysis of the mixture subjected to 60 minutes of advanced grinding

Size distribution profiles of the advanced milled powder particles were also determined with the use of the DLS method. Particle sizes were measured at 23 °C. Cumulative results are given below each figure. Based on DLS analysis (cumulative results), it can be seen that after 15 minutes of further grinding, more than 80% of the material is below 9460 nm, after 30 minutes of grinding is 5240.2 nm, and after 60 minutes of grinding is 6024.9 nm. It can be seen that the results obtained from SEM analysis and the DLS method are comparable.

3.2. SEM/EDX Analyses

SEM images of the samples were taken after the advanced grinding process. According to the image in Figure 9 (a), most of the material has been ground down to sub-micron and has even started to clump. However, it is noteworthy that there are some grains that are not coarsely ground and whose crystal structure is not amorphous. It can be said that these grains are quartzite grains.

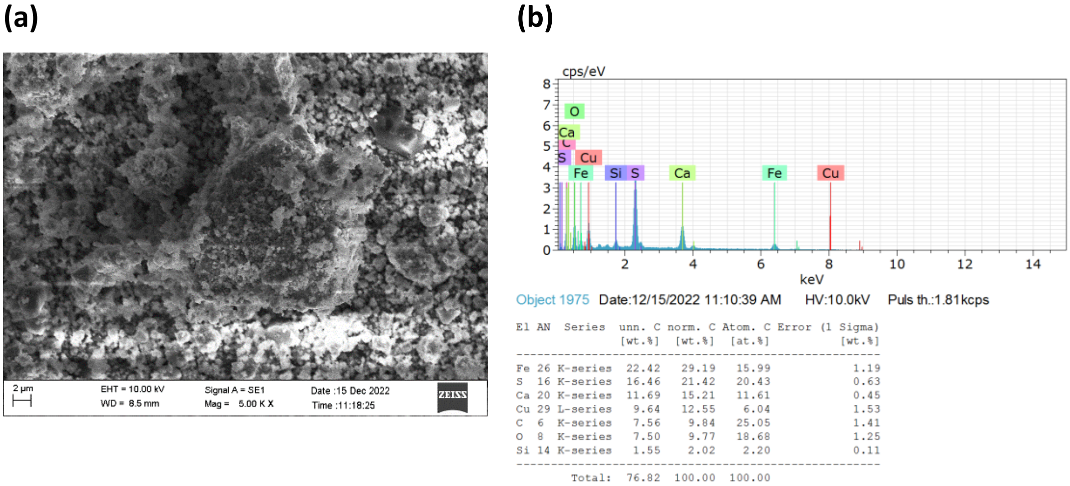

Figure 9. (a) SEM (x5000) and (b) EDX images of the sample subjected to 15 minutes of grinding

Figure 10 (a) and (b) and Figure 11 (a) and (b) show the SEM and EDX images of the samples that were subjected to advanced grinding for 30 minutes and 60 minutes, respectively.

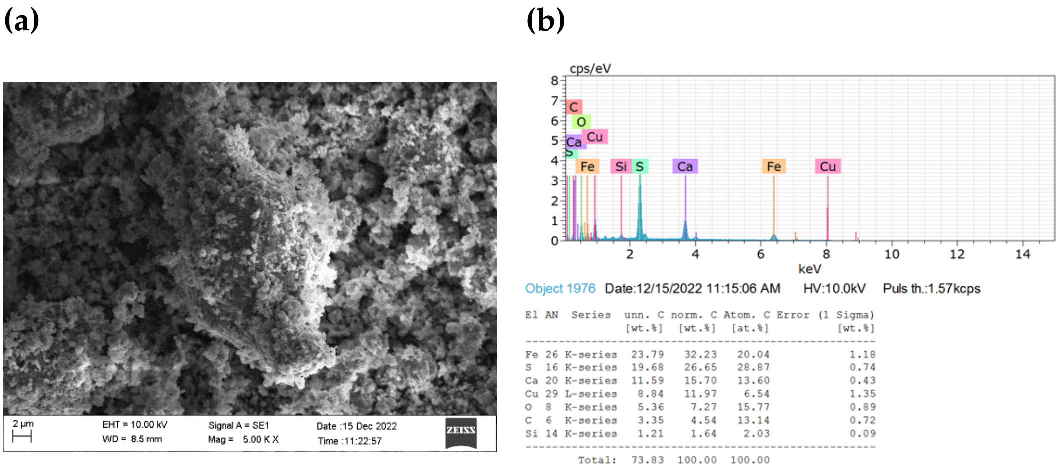

Figure 10. (a) SEM (x5000) and (b) EDX images of the sample subjected to 30 minutes of grinding

(a) (b)

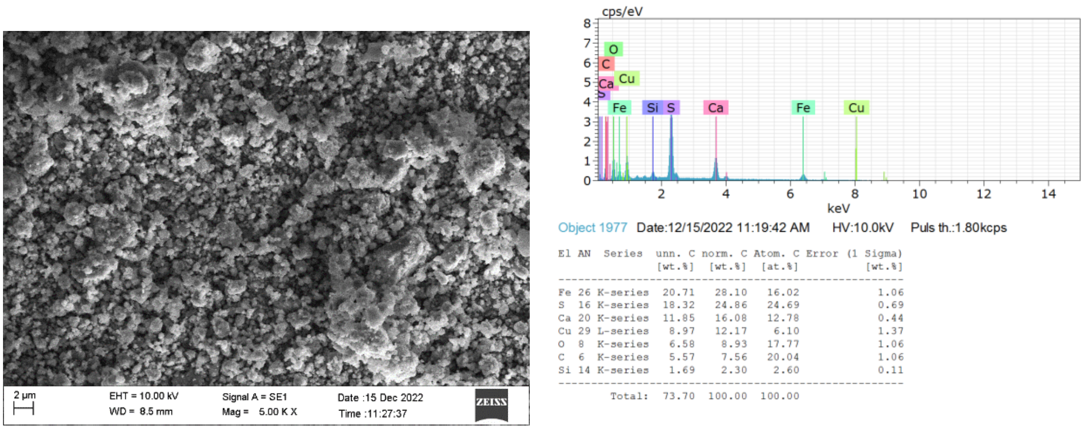

El	AN	Series	unn. C [wt.%]	norm. C [wt.%]	Atom. C [at.%]	Error (1 Sigma) [wt.%]
Fe	26	K-series	20.71	28.10	16.02	1.06
S	16	K-series	18.32	24.86	24.69	0.69
Ca	20	K-series	11.85	16.08	12.78	0.44
Cu	29	L-series	8.97	12.17	6.10	1.37
O	8	K-series	6.58	8.93	17.77	1.06
C	6	K-series	5.57	7.56	20.04	1.06
Si	14	K-series	1.69	2.30	2.60	0.11
		Total:	73.70	100.00	100.00	

Figure 11. (a) SEM (x5000) and (b) EDX images of the sample subjected to 60 minutes of grinding

When Figure 10 (a) and (b) and Figure 11 (a) and (b) are examined, it is understood that most of the material has gone below micron, and the grains that started to clump after 15 minutes of grinding are dispersed again.

3.3. TG/DTA Analyses

Thermo-gravimetric analysis (TG) is a technique that records the change in mass of the sample as a function of temperature. In the differential thermal analysis (DTA) method, the same temperature program is applied to the sample and a thermally inert reference material, and the difference between the two is measured as a function of temperature. These two substances are heated together by increasing the temperature smoothly. Dehydration, decomposition, melting, evaporation and sublimation events are endothermic, while amorphization, crystallization from amorphous state, solidification, formation of a new crystal structure from the crystal structure are exothermic [23].

TG/DTA curves characterizing the behavior of the original mixture against thermal effect are given in Figure 12.

(a) (b)

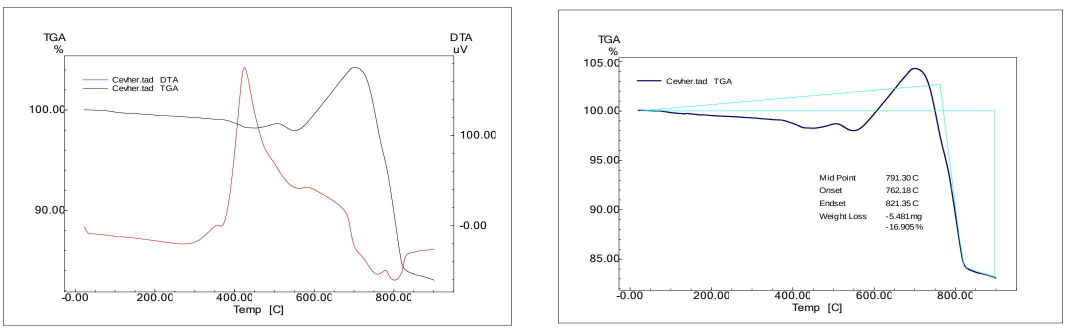

Figure 12. a) TG/DTA analysis, b) TGA analysis peak values of the original sample (taken in air)

In the TG/DTA images given in Figure 12 (a), it is seen that endothermic reactions occur in the mixture, starting at 380 ^oC and continuing up to 700 ^oC, and exothermic reactions begin and continue after 700 ^oC. These analyses performed in the atmospheric environment show that the oxygen in the air reacts with the sulphur in the chalcopyrite, therefore, first there is an increase in weight and endothermic reactions take place until the ignition temperature of the sulphur, and then exothermic reactions begin as a result of the burning of the sulphur. At a temperature of approximately 400 ^oC, the burning of carbon begins. When the TGA values given in Figure 12 (b) are examined, it is seen that the sample has lost approximately 16.905% weight.

For the temperatures at which TG/DTA analyses were taken, it is stated in the literature that the reactions and fundamental changes occurring can be explained by the following reactions. Pyrite decomposes according to the reaction (3.1) around 200-300 ^oC.

$$FeS_{2(s)} \rightarrow FeS_{(s)} + 1/2S_{2(g)} \quad (3.1)$$

Thermal decomposition of chalcopyrite occurs according to equation (3.2) and yields elemental sulphur.

$$2CuFeS_{2(s)} \rightarrow Cu_2S_{(s)} + 2FeS_{(s)} + 1/2S_{2(s)} \quad (3.2)$$

Covellin (CuS), on the other hand, breaks down at 358 ^oC, releasing sulphur, according to equation (3.3).

$$2CuS_{(s)} \rightarrow Cu_2S_{(s)} + 1/2\ S_{2(g)} \quad (3.3)$$

All of these reactions are endothermic and require external energy. After these reactions, oxidation reactions begin to occur, and sulphur elimination reactions begin, all of which are exothermic [35]. According to TG/DTA analyses of the original sample in air, these endothermic reactions appear to occur between approximately 300-700 ^oC. The increase in weight after 400 ^oC can be said that iron sulphide and copper sulphide compounds reacting with the oxygen of the air are oxidized, first causing an increase in weight, and then with the start of exothermic reactions, these oxidized structures move away from the body, causing a decrease in weight. In the literature, it is stated that sulphation reactions occur directly between sulphur and oxygen, not through oxides, and that copper sulphate formation starts at 350 ^oC and is maximum at 550 ^oC, and that $CuSO_4$ and CuO can combine to form basic sulphate ($CuO.CuSO_4$) around 500 ^oC. It is claimed that sulphate will decompose into basic sulphate at 650 ^oC, and will turn into CuO and SO_3 at 700 ^oC with the increase in temperature [35].

According to reactions (3.4) and (3.5), sulphates break down and cause the formation of ferrites. Copper ferrite formation begins at 600 ^oC. Further increase in temperature causes the formation of $Cu_2O.Fe_2O_3$, which is a stable compound above 1100 ^oC.

$$FeSO_4 + Fe_2O_3 \rightarrow FeO.Fe_2O_3 + SO_3 \quad (3.4)$$

$$CuSO_4 + Fe_2O_3 \rightarrow CuO.Fe_2O_3 + SO_3 \quad (3.5)$$

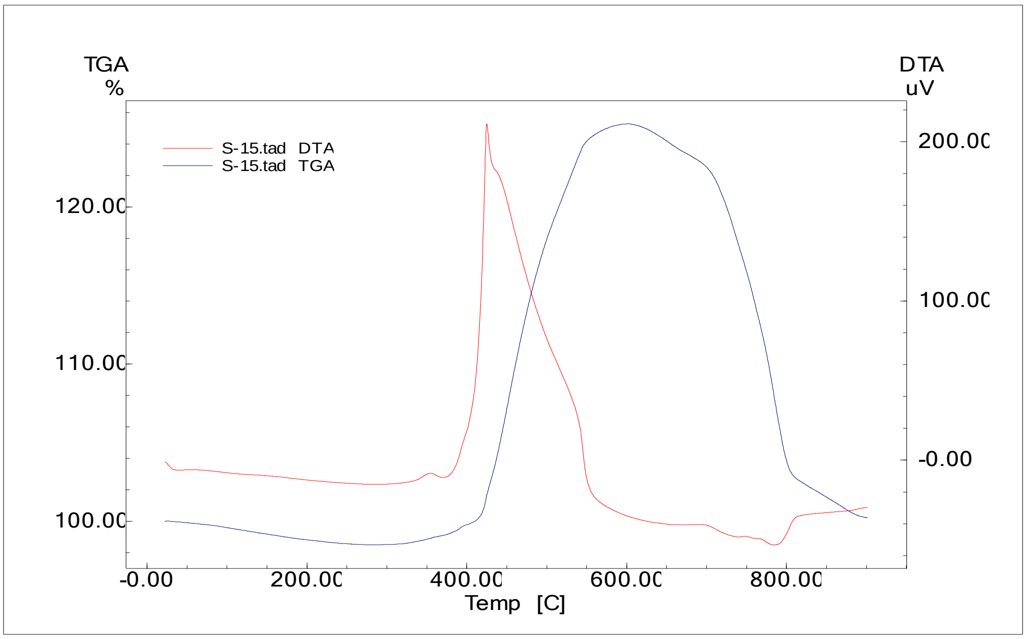

Figure 13. TG/DTA analysis of the sample subjected to advanced grinding for 15 minutes

TG/DTA analysis of the sample subjected to 15 minutes of advanced grinding is given in Figure 13. When chalcopyrite is mixed with calcium oxide and carbon and then subjected to heat treatment, the sulphur of chalcopyrite will combine with calcium according to reaction (2.1), and calcium sulphide, iron oxide, carbon monoxide and metallic copper will be released. When the released carbon monoxide molecules collide with the chalcopyrite particles in the medium without coming into contact with the oxygen of the air, the reaction (3.6) may also partially occur.

$$CuFeS_{2(s)} + 2CaO_{(s)} + C_{(s)} = Cu_{(s)} + FeO_{(s)} + 2CaS_{(s)} + CO_{(g)} \tag{2.1}$$

$$CuFeS_{2(s)} + 2CaO_{(k)} + CO_{(s)} = Cu_{(s)} + FeO_{(s)} + 2CaS_{(s)} + CO_{2(g)} \tag{3.6}$$

In this case, we can say that the reactions that sulphur gave in the original sample (Figure 12 (a) and (b)) did not occur here. Here, sulphur is held by CaO and CO_2 or CO gas is released into the environment. Therefore, weight loss will remain low depending on the amount of carbon added in stoichiometric ratio.

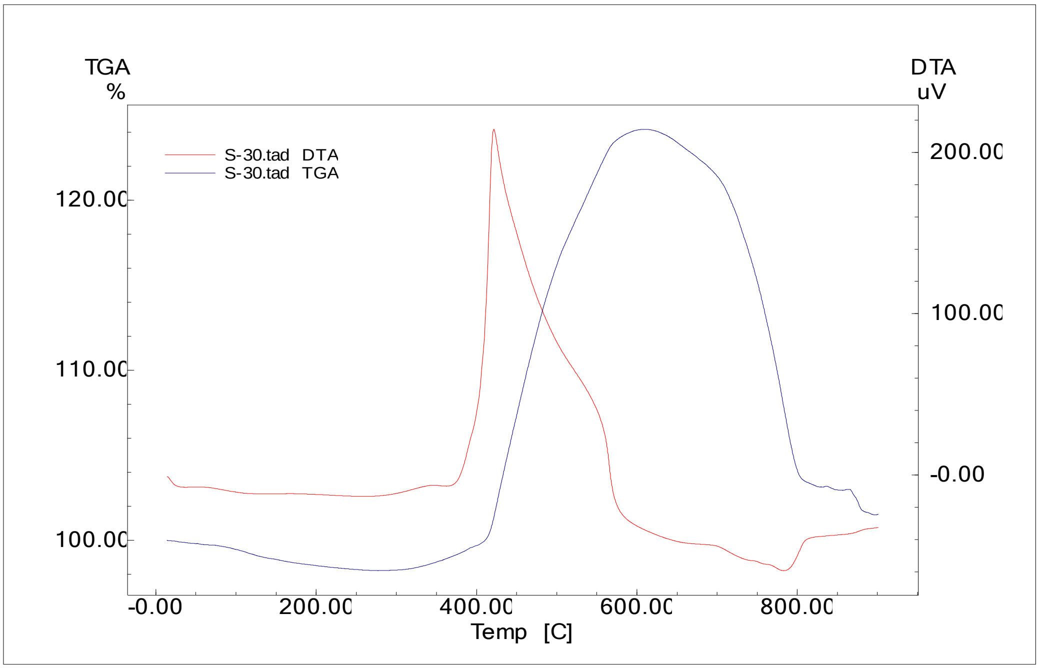

Figure 14. TG/DTA analysis of the sample subjected to advanced grinding for 30 minutes

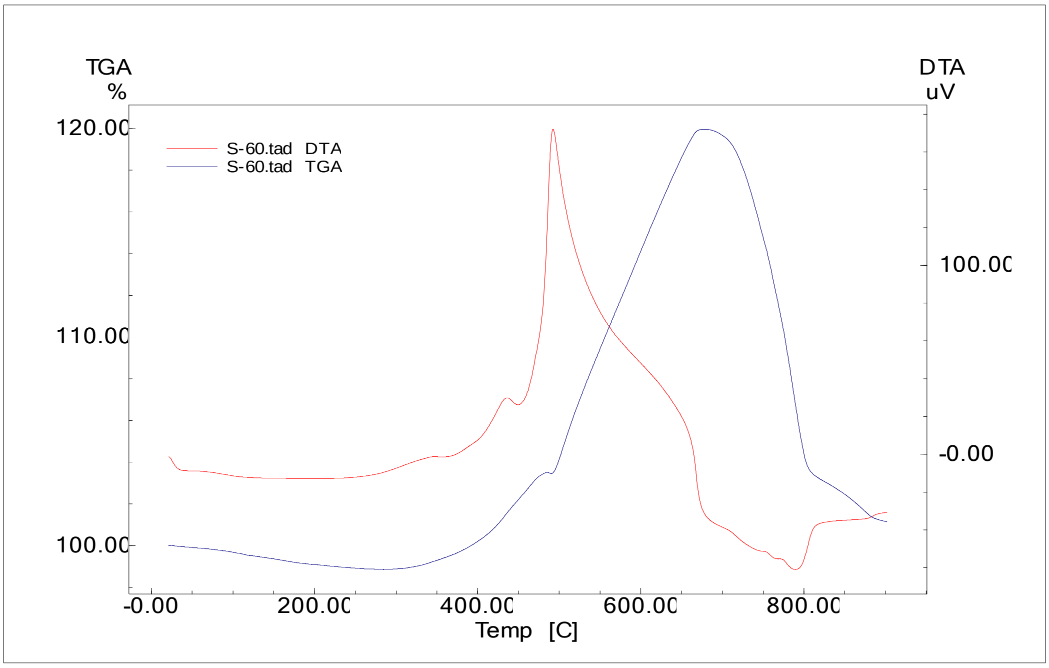

Figure 15. TG/DTA analysis of the sample subjected to advanced grinding for 60 minutes

Figure 14 and Figure 15 show the TG/DTA analyses of the samples that were subjected to advanced grinding for 30 minutes and 60 minutes, respectively. When the images are examined, it can be said that after an almost 20% weight increase that started with endothermic reactions, an exothermic reaction started (~620 ^oC) and a tendency to decrease in weight started from this temperature. However, the total weight loss was not as in the original sample and remained lower. We can attribute the low weight loss to equation (2.1) above.

4. Conclusion

In this study, the changes in the physical structure of a mixture consisting of biocoal-chalcopyrite concentrate and quicklime, prepared for the direct reduction of chalcopyrite, were examined as a result of subjecting it to the advanced grinding process.

Biocoal, chalcopyrite concentrate and quicklime (CaO) were blended in a stoichiometric ratio and subjected to further grinding in a spex mill. With the further grinding process, it was observed that the dominant peak of chalcopyrite in the original sample decreased depending on the further grinding time. It was concluded that the formation of nanostructures through grinding processes triggered this. Especially after 30 minutes of grinding, it is seen that 80% of the material falls below 5 µm. It was concluded that the powders in the concentrate were affected by these temperature increases as a result of both the local temperatures resulting from the collision of the balls with each other and the powder material during grinding, and the temperatures created by the balls hitting the walls in the chamber, and the crystal structure was deteriorated. However, it was observed that the silicate structure remained intact.

When TG/DTA analyses were examined, it was seen that after an almost 20% weight increase that started with endothermic reactions, an exothermic reaction started (~620 ºC) and a tendency to decrease in weight began from this temperature. However, the total weight loss was not as in the original sample and remained lower.

This study constitutes the first part of the studies on the direct reduction of chalcopyrite with carbon. In the ongoing part of the study, a study investigating the effect of advanced grinding processes on the direct reduction of chalcopyrite concentrate with carbon and quicklime will be presented.

Acknowledgments

This study was covered from “Effect of Mechanical Activation on the Direct Reduction of Chalcopyrite Concentrate with Carbon” titled the master’s thesis.

Conflict of Interest

Authors approve that to the best of their knowledge, there is not any conflict of interest or common interest with an institution/organization or a person that may affect the review process of the paper.

Research and Publication Ethics Statement

The authors declare that this study complies with research and publication ethics.

References

[1] Habashi, F. (1978). Chalcopyrite: Its Chemistry and Metallurgy. New York (McGraw Hill), ISBN 0-07-025383-8.

[2] Boyrazlı, M. (2001). Bakır Konverter Cürufunun Dikromatlı Ortamda Liçinin İncelenmesi, Fırat Üniversitesi, Fen Bilimleri Enstitüsü, Yüksek Lisans Tezi

[3] Özboz, F., Kartal, M., Alp, A. (2016). Karadeniz Rize Bölgesi Bakır Sülfür Cevherlerinin Anodik Oksidasyon Prosesi ile Liçi ve Çevre Açısından Önemi, I*SEM2016, 3rd International Symposium on Environment and Morality*, 4-6 November 2016, Alanya-Antalya/Turkey

[4] Santoro, S., Estay, H., Avci, A. H., Pugliese, L., Ruby-Figueroa, R., Garcia, A., Aquino, M., Nasirov, S., Straface, S., Curcio, E. (2021). Membrane technology for a sustainable copper mining industry: The Chilean paradigm. *Cleaner Engineering and Technology*, 2, 100091.

[5] Hawker, W., Vaughan, J., Jak, E., Hayes, P.C. (2017). The Synergistic Copper Process concept, *Mineral Processing and Extractive Metallurgy IMM Transactions Section C*

[6] Jha, A., Grieveson, P., Jeffes, JHE. (1989) An investigation on the carbothermic reduction of copper sulfide minerals-kinetic and thermodynamic considerations. *Scandinavian Journal of Metallurgy* 18.1, 31-45.

[7] Moinpour, M., Rao, YK. (1985) Direct reduction of copper sulfide with carbon in the presence of lime, *Canadian Metallurgical Quarterly*, 1985: Vol. 24, No. 1, pp. 69-81.

[8] Machingawuta, N., Jha, A., Grieveson, P. (1989) Mechanism of carbothermic reduction of nickel sulfide minerals in the presence of lime, *Scandinavian Journal of Metallurgy*, 18, pp. 81-88.

[9] El-Rahaiby, S.K., Rao, Y.K. (1984) Cell measurements of the reduction potentials of gas-phase emanating from PbS/CaO/C at elevated temperatures, *Metall. Trans.* 15B, 19.

[10] Bronson, M.C., Sohn H.Y. (1983) The carbothermic reduction of nickel sulfide in the presence of lime, *Metallurgical Transaction B*, Vol. 14B, December, pp. 605-615.

[11] Terry, B.S., Riveros, G., Sanchez, M., Jeffes, J.H.E. (1984) Lime-concentrate process for roasting of copper-bearing sulphides-part 1 : analysis of optimum roasting conditions, *Trans. Instn Min. Metall.* (Sec. C: Mineral process, Extr. Metall.), 103, C193-200.

[12] Terry, B.S., Riveros, G., Sanchez, M., Jeffes, J.H.E. (1984) Lime-concentrate process for roasting of copper-bearing sulphides-part 2: effect of sulfide: lime ratio, air flow rate, pellet size and porosity on reaction kinetics, *Trans. Instn Min. Metall.* (Sec. C: Mineral process, Extr. Metall.), 103, C201-209.

[13] Terry, B.S., Riveros, G., Sanchez, M., Jeffes, J.H.E. (1984) Lime-concentrate process for roasting of copper-bearing sulphides-part 3: mechanism of roasting reactions, *Trans. Instn Min. Metall.* (Sec. C: Mineral process, Extr. Metall.), 103, C210-216.

[14] Vahdati Khaki, J., Hadji Soleimani, S., Moosavi Nejad M. (2007) Direct Reduction of Sarcheshme Copper Sulfide Concentrate with Carbon in The Presence of Lime, *Iranian Journal of Materials Science and Engineering*, Vol. 4, Numbers 1 and 2, winter and spring 2007

[15] Yılmaz, T., Alp, İ., Deveci, H., Duran, C., Celep, O. (2007). Kayabaşı Masif Bakır Cevherinin Ferrik Sülfat Liçi, İstanbul Üniversitesi, *Yerbilimleri Dergisi*, 2007;20:63-69.

[16] Xiao, L., Fang, Z., Qiu, G.Z., Wang, S.F., Wang, C-X. (2010). Mechanism of Electro-Generative-Leaching of Chalcopyrite-MnO_2 in Presence of Acidithiobacillus Ferrooxidans, *Trans.Nonferrous Met. Soc. China* 2010;20:15-20.

[17] Eghbalnia, M., Dixon, D.G. (2011) Electrochemical Study of Leached Chalcopyrite Using Solid-Paraffin-Based Carbon Paste Electrodes, *Hydrometallurgy*, 2011;110:1–12.

[18] Arancı, E. (2014) Mekanik aktivasyon işlemine tabi tutulmuş demirli mangan oksit cevherinden karbotermik yöntemle ferromangan üretimine karbonize çay atıklarının etkisi, Fırat Üniversitesi / Fen Bilimleri Enstitüsü / Metalurji ve Malzeme Mühendisliği Ana Bilim Dalı, Yüksek Lisans Tezi

[19] Baláž, P., et al. (2013) Hallmarks of mechanochemistry: from nanoparticles to technology. *Chemical Society Reviews* 42.18 pp. 7571-7637.

[20] Apaydin, F., Atasoy, A., Yildiz, K. (2011). Mekanik Aktive Edilmiş Kromitin Grafitle Karbotermal Redüksiyon Kinetiği, *SAÜ. Fen Bilimleri Dergisi*, 15. Cilt, 1. Sayı, s.17-22.

[21] Demir, F., Algül, H., Gül, H., Akçil, M., Alp, A. (2021). Mekanik Aktivasyon Yapılmış Çinko Konsantrelerinde Kavurma Sıcaklığının Redüksiyonuna Etkisinin Termal Analiz Yöntemleri ile İncelenmesi, *Academic Platform Journal of Engineering and Science* 9-2, 324-331.

[22] Uysal, T., Erdemoğlu, M., Birinci, M. (2019). Pirofillit Cevherinden Asit Liçi Yöntemiyle Alüminyum Kazanımına Aktivasyonun Etkisi, *Madencilik*, 2019, 58(2), 111-120.

[23] Arancı, E.Ö. (2018). Manyetit Cevheri Konsantresinin Karbonize Çay Tesis Atıkları ile Mikrodalga Redüksiyonuna Mekanik Aktivasyon İşleminin Etkisinin Araştırılması. Fırat Üniversitesi, Metalurji ve Malzeme Mühendisliği Anabilim Dalı, Doktora Tezi.

[24] Perek, K.T., Arslan, F. (2010). Effect of Mechanical Activation on Pressure Leaching of Küre Massive Rich Ore, *Mineral Processing and Extractive Metallurgy Review*, No. 31, 2010, s. 191-200, ISSN: 0882-7508, Taylor&Francis

[25] Baláž, P. (2003). Mechanical activation in hydrometallurgy, *International Journal of Mineral Processing* 72.1-4 pp. 341-354

[26] Çakır, M. (2010). Bakır Atıklarından Bakır Kazanımına Mekanik Aktivasyonun Etkisi, Sakarya Üniversitesi, Fen Bilimleri Enstitüsü, Yüksek Lisans Tezi

[27] Demirel, S. (2011). Rize Bölgesi Bakır Cevherlerinden Bakır Kazanımına Mekanik Aktivasyonun Etkisi, Sakarya Üniversitesi, Fen Bilimleri Enstitüsü, Yüksek Lisans Tezi

[28] Türkiye İstatistik Kurumu Verileri, https://biruni.tuik.gov.tr/

[29] Bulut, Y., Tez Z. (2007). Adsorption studies on ground shells of hazelnut and almond. *J. Hazard. Mater.*, 149, 35-41, 2007

[30] Hasar, H., Cuci, Y. (2000). Removal of Cr(VI), Cd(II), and Cu(II) by Activated Carbon Prepared from Almond Husk", Enviromental Technology, Vol. 21, No. 12, pp. 1337-1342(6), 1 December 2000

[31] Urrestarazu, M., Salas, M.C., Matarin, A., Martinez, G., Segure, M.L. (2004). Almond Waste: A New Ecology-Friedly Alternative Substrate in Tomato Culture. *Acta Hort.* (ISHS) 638:285-288.

[32] Özsin, G. (2018). Termal analiz ile birleştirilmiş spektral yöntemlerin kullanımı ile biyokütle pirolizinin incelenmesi. *BAUN Fen Bil. Enst. Dergisi*, 20(2), 315-329.

[33] Boyrazlı, M., Arancı, E.Ö., Şengül, N., Çelik, T., Abo, A. (2019). Badem Kabuklarının Karbonizasyonu, MAS European International Congress On Mathematics-Engineering-Natural & Medical Sciences-VIII, October 11-13, 2019, Diyarbakır, Turkey.

[34] https://rruff.info/chalcopyrite/display=default/

[35] Bor, F.Y. (1989) Ekstraktif Metalurji Prensipleri-Kısım:2. İTÜ Matbaası, 1989.